

## RESEARCH ARTICLE

# Study on Optical Fiber Gas-Holdup Meter Signal Denoising Using Improved Threshold Wavelet Transform

SHENGXUE DU<sup>1</sup> AND SHUJUN CHEN<sup>2</sup><sup>1</sup>School of Information and Electrical Engineering, Hebei University of Engineering, Handan 056038, China<sup>2</sup>Educational Technology Center, Hebei University of Engineering, Handan 056038, China

Corresponding author: Shengxue Du (shxdu2013@126.com)

This work was supported in part by the Doctoral Initiation Fund of Hebei University of Engineering under Grant SJ220100319.

**ABSTRACT** The optical fiber probe gas-holdup meter is a new logging tool, which can be used to measure the gas-holdup of oil-gas-water three-phase flow during production logging. In this paper, the wavelet transform is used to denoise the measured gas-holdup signal of the optical fiber probe. For the wavelet transform threshold de-noising method, the existing hard and soft threshold functions have certain defects. So we propose a wavelet transform denoising method with an improved threshold function, and use this method to denoise the measured gas-holdup signal of the optical fiber probe. The signal-to-noise ratio, root mean square error, smoothness, and correlation coefficient are used as the evaluation indexes of signal denoising effect. The improved threshold function is between the hard threshold function and the soft threshold function. It has the advantages of both hard and soft threshold functions, can effectively overcome the discontinuity of the hard threshold function and the constant deviation of the soft threshold function, and improves the denoising efficiency of the gas-holdup signal. The proposed method is applied to the synthetic data and the real gas-holdup signal of the optical fiber probe respectively. Compared with the traditional soft and hard threshold functions, the experiment results show that the improved threshold wavelet denoising method is feasible. And it is effective in the gas-holdup signal denoising, improving the signal-to-noise ratio, reducing root mean square error, and increasing the correlation coefficient. The proposed method preserves well the original features of the measured gas-holdup signal, which provides a reference for the signal processing and dynamic monitoring analysis of the subsequent oil-well downhole development.

**INDEX TERMS** Improved threshold function, wavelet threshold, optical fiber gas-holdup meter, denoising, gas-holdup.

**NOMENCLATURE**

$ca_i$	The low-frequency part of the $i$ th layer, after the wavelet transform decomposition.
$cd_i$	The high-frequency part of the $i$ th layer, after the wavelet transform decomposition.
$db8$	The wavelet basis function.
$e(t)$	The noise at moment $t$ .
$f(t)$	The pure signal at moment $t$ .
$Heursure$	A thresholding selection rule.
$Minimaxi$	A thresholding selection rule.

$n$	The length of the signal.
$N$	The total levels of wavelet transform decomposition.
$r$	An evaluation index: the smoothness.
$R$	An evaluation index: the correlation coefficient.
$Rigrsure$	A thresholding selection rule.
$RMSE$	The root mean square error.
$s$	The noisy signal.
$\hat{s}$	The denoised signal.
$SNR$	The signal-to-noise ratio.
$Sqtwolog$	A thresholding selection rule.
$s(t)$	The noisy signal at moment $t$ .

The associate editor coordinating the review of this manuscript and approving it for publication was Baoping Cai<sup>1</sup>.

$\hat{s}(t)$	The denoised signal at moment $t$ .
$V_{REF+}$	The high value of reference voltage.
$V_{REF-}$	The low value of reference voltage.
$w$	The high-frequency coefficient vector after a wavelet transform decomposition.
$\hat{w}$	The high-frequency coefficient vector after threshold processing.
$\omega_{i,j}$	The $i$ th coefficient of the $j$ th layer after a wavelet transform decomposition.
$w_{ij}$	The $i$ th coefficient of the $j$ th layer after threshold processing.
$XWT$	The cross-wavelet transform.
$\lambda$	The selected threshold.
$\sigma$	The noise coefficient.

## I. INTRODUCTION

In the middle and late stages of oilfield development, there is a large amount of formation water in the oil layer. Hence, the oil produced from the oil well is often not a single crude oil but a mixture of crude oil, natural gas, and water, resulting in a complex situation of the three-phase mixed flow of oil, gas, and water in the vertical rising pipe diameter. The gas-holdup in oil-gas-water three-phase flow [1], [2] refers to the proportion of gas phase in the mixed fluid. Therefore, real-time dynamic monitoring of oil well production is carried out, and the gas holdup is a significant parameter in multiphase fluid flow. At present, the theoretical calculation model has excellent limitations. Experimental measurement is the principal means to study the gas holdup, and it is also an essential means to research the three-phase flow of oil-gas-water. A variety of methods for measuring gas holdup have been developed at home and abroad, such as the fast closing valve method, conductivity probe method, capacitance method [3], ray method, ultrasonic method [4], high-speed photography, etc. Still, each of these methods has its limitations and particular pertinence. The use of an optical fiber probe [5] to measure the local gas content of oil, gas, and water three-phase flow is an advanced measurement method. This method has many advantages, such as low loss, wide frequency band, thin wire diameter, lightweight, insulation, anti-electromagnetic interference, corrosion resistance, good dehumidification effect, high sensitivity, convenient signal processing, etc. It can meet the needs of real-time measurement of oil-gas-water three-phase fluid in the well [6].

As the signal of the optical fiber gas-holdup meter changes with the detection state and time, on the one hand, it has prominent non-stationary characteristics; on the other hand, there are many noise interferences, such as mode noise, Gaussian noise, band limiting white noise, shot noise, thermal noise, etc. Reference [7] generated by three modules, such as the sensing system, photoelectric conversion, and signal acquisition system, which affect the quality of the signal. It may even cover the characteristic information of weak signals generated by tiny bubbles in the fluid, making it difficult to process the signals correctly.

Traditional signal analysis and processing techniques are based on Fourier analysis, which cannot express the time-frequency local performance of the signal. In recent years, some noise reduction techniques have been proposed based on different mode decomposition algorithms. The empirical mode decomposition (EMD) denoising properties were addressed soon after the introduction of the method, and they are reported in [8] and [9]. As an empirical signal analysis method, EMD overcomes the limitation of the Fourier transform fundamentally and can theoretically decompose any signal into IMFs [10]. Subsequently, EMD was effectively used for signal denoising in a wide range of applications, such as biomedical signals [11], acoustic signals [12], ionospheric signals [13], and underwater acoustic signals [14]. Han and van der Baan use ensemble empirical mode decomposition and adaptive thresholding for microseismic denoising. However, these methods are either not very effective for removing high-amplitude noise of surface microseismic data without distorting emergent arrivals of the signals, or they are not fully automated and have parameters that need to be tuned manually [15].

The wavelet transform method is developed based on Fourier analysis and short-time Fourier analysis [16]. Wavelet transform can multi-scale refine the signal by calculating flex and transition, which solves the problem that the size of the Fourier transform window cannot change with frequency. The wavelet transform is a popular time-frequency transform [17]. It produces a time-frequency representation with better resolution compared with the short-time Fourier transform [18], because the signal is analyzed under different resolutions (or scales) at different frequencies. The idea behind the wavelet transform is to apply a prototype analyzing function known as the mother wavelet over the time series. Depending on what signal features are of interest, a wavelet can be selected to facilitate the detection of that feature. Wavelet transforms are powerful mathematical functions that analyze data according to scale or resolution. They provide many advantages over Fourier transforms [19]. For example, they handle well approximating signals with sharp spikes or signals having discontinuities. Hence, for handling non-stationary signals like seismic data, Fourier has been virtually outdated by wavelet [20]. To et al. [21] have compared the traditional Wiener filtering in the Fourier domain and threshold-based wavelet techniques and proved the wavelet-based denoising algorithm had outperformed the Wiener filtering in denoising the micro-seismic signals. Puneet K J [22] proposed an adaptive threshold estimation method and a nonlinear medium threshold function for ECG signal de-noising based on a wavelet. It showed that it could effectively suppress various types of noises and noises. Anestis and Oppenheim [23] and Ansari et al. [24] have used wavelet denoising on high noise signals and proved its efficiency over the conventional filtering technique. At present, wavelet transform is widely used for signal denoising in practical engineering applications because of its advantages, such as easy implementation, complete preservation of original signal features, etc.

In this paper, the wavelet transform is used to denoise the measured gas-holdup signal of the optical fiber probe. Using the multi-scale and multi-resolution characteristics of the wavelet transform, the signal of the optical fiber gas holdup meter is decomposed, and the signals of different frequency bands are displayed on different scales of the wavelet decomposition. To correctly reflect the characteristic parameters of oil-gas-water three-phase flow, and obtain the desired local gas holdup value of oil-gas-water three-phase flow, during signal reconstruction, the information on the scale of high-frequency interference is removed, so that the reconstructed signal no longer contains interference components. The wavelet transform threshold processing mainly includes hard threshold function denoising and soft threshold function denoising. Because the traditional threshold function is discontinuous or continuous but not smooth at the threshold point. To solve these problems a wavelet denoising method based on the improved threshold function is proposed in this paper. The threshold function is between the soft and hard thresholds, which can well retain useful signals, and improve the performance of the threshold function. In the experiment part, the proposed method is respectively used to denoise the synthetic signal and the measured signal of the optical fiber probe gas-holdup meter to verify the validity of the method. The proposed method is also compared with other methods in signal denoising effect, and several indicators are used to evaluate the denoising effect: signal-to-noise ratio, root mean square error, smoothness, and correlation coefficient. On this basis, the cross-wavelet transform method (XWT) is used to further evaluate the denoising effect of this method.

The rest of this article is organized as follows. Section II introduces the basic theory of wavelet threshold denoising. Section III proposes the wavelet transform denoising method based on an improved threshold function and provides the evaluation indexes of the denoising effect. Section IV designs the experiment projects and analyzes the experiment results. Finally, Section V concludes this article.

## II. THEORY OF WAVELET THRESHOLD DE-NOISING

Suppose that the useful signal  $f(t)$  becomes  $s(t)$  after being interfered by noise, then the basic signal model can be expressed as:

$$s(t) = f(t) + \sigma e(t), \quad t = 0, 1, 2, \dots, n - 1 \quad (1)$$

where  $e(t)$  is the noise,  $\sigma$  is a noise correlation coefficient. In the simplest case,  $e(t)$  can be assumed to be a Gaussian white noise and  $\sigma = 1$ . In practical engineering, the useful signal  $f(t)$  is usually a low-frequency signal or relatively stable signal, and while noise signals are often high-frequency signals. The purpose of wavelet transform is to suppress the useless part  $e(t)$  of the signal and restore the useful part  $f(t)$ . When the decomposition coefficient of  $f(t)$  is sparse, this method is very efficient.

The wavelet threshold denoising process includes the wavelet transform decomposition, threshold processing, and signal reconstruction. Its principle is shown in Fig. 1.

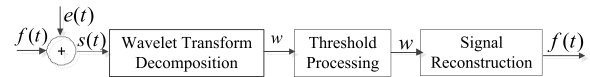


FIGURE 1. Wavelet threshold de-noising principle.

Wavelet threshold filtering is to compare wavelet coefficients with a given threshold. If the wavelet coefficients are smaller than the threshold, the wavelet coefficients are set to zero. If the wavelet coefficient is larger than that threshold, the wavelet coefficient shall be retained or modified. The commonly used threshold functions are the hard threshold function and the soft threshold function.

The soft threshold filtering function is:

$$\hat{\omega}_{i,j} = \begin{cases} \text{sign}(\omega_{i,j}) (|\omega_{i,j}| - \lambda), & |\omega_{i,j}| \geq \lambda \\ 0, & |\omega_{i,j}| < \lambda \end{cases} \quad (2)$$

The hard threshold filtering function is:

$$\hat{\omega}_{i,j} = \begin{cases} \omega_{i,j}, & |\omega_{i,j}| \geq \lambda \\ 0, & |\omega_{i,j}| < \lambda \end{cases} \quad (3)$$

In (2) and (3),  $\omega_{i,j}$  is the  $i$ th coefficient of the  $j$ th layer of the wavelet transform of the noisy signal, and  $\hat{\omega}_{i,j}$  is the corresponding wavelet coefficient after threshold processing,  $\lambda$  indicates the selected threshold.

The wavelet threshold transform method is generally divided into the following three steps:

① The noisy signal is decomposed by a wavelet transform. According to the characteristics of the signal, a proper wavelet basis function and the decomposition level  $N$  are selected. And the noisy signal is decomposed into  $N$  layers of wavelet. The choice of decomposition level  $N$  depends on the amount of noise signal in the signal. More noise requires more decomposition levels, while less noise requires fewer decomposition levels. For example, 3-layer wavelet decomposition is performed on the noisy signal  $s$ , and the decomposition process is shown in Fig. 2.

In Fig. 2, after the first layer decomposition of the signal  $s$ ,  $ca_1$  is the approximate value of  $s$ , and  $cd_1$  is the detail of  $s$ . By analogy,  $ca_1$  is decomposed into the second layer, and there are three layers in total. The decomposed signal  $s$  can be expressed as:

$$s = ca_3 + cd_3 + cd_2 + cd_1 \quad (4)$$

In (4),  $ca_3$  is the low-frequency part after a signal decomposition, which basically contains the main components of the effective signal.  $cd_1$  to  $cd_3$  are mainly high-frequency parts, including high-frequency parts of effective signal conversion and the wavelet coefficients generated by noise.

② Threshold quantization of wavelet decomposition high-frequency coefficients. According to a threshold quantization criterion, for each layer of high-frequency coefficients from layer 1 to layer  $N$ , a reasonable threshold function is selected to modify the wavelet coefficients  $w$ , and the estimated wavelet coefficients  $\hat{w}$  are obtained by threshold quantization.

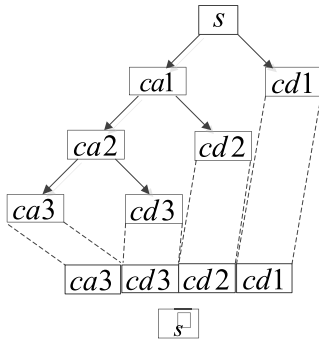


FIGURE 2. Three layers wavelet decomposition of the signal.

③ Signal reconstruction. The high-frequency wavelet coefficients  $w$  from the first layer to the  $N$ -th layer after threshold quantization and the low-frequency wavelet coefficients from the  $N$ -th layer are implemented with an inverse wavelet transform to obtain the estimated signal  $\hat{s}(t)$ , which is the effective signal after the noise reduction.

### III. BASED ON IMPROVED THRESHOLD FUNCTION DE-NOISING FOR GAS-HOLDUP SIGNAL OF OPTICAL FIBER PROBE

#### A. EVALUATION OF SIGNAL DE-NOISING EFFECT

In the field of signal denoising, 2 indicators are widely used to evaluate the effect of signal denoising: the output signal-to-noise ratio ( $SNR$ ) and the root mean square error ( $RMSE$ ).

$$SNR = 10 \lg \left\{ \frac{\sum_{t=1}^{t=n} s^2(t)}{\sum_{t=1}^{t=n} [s(t) - \hat{s}(t)]^2} \right\} \quad (5)$$

$$RMSE = \left\{ (1/n) \sum_{t=1}^{t=n} [s(t) - \hat{s}(t)]^2 \right\}^{1/2} \quad (6)$$

where,  $s(t)$  is the original signal,  $\hat{s}(t)$  is the output signal after noise reduction, and  $n$  is the length of the signal.

According to the definition,  $SNR$  is actually the ratio between the original signal and the noise energy. It is a common method to detect the noise component in the signal. The larger the  $SNR$  value, the smaller the proportion of noise components in the signal, and the better the denoising effect.  $RMSE$  refers to the root mean square error between the original signal and the signal after noise removal and reconstruction. The root mean square error reflects the similarity between the original signal and the signal after noise removal and reconstruction, and can be used as the evaluation index of the original signal restoration degree of the signal after noise removal and reconstruction. The smaller the  $RMSE$  value, the higher the similarity between the de-noised reconstructed signal and the original signal, and the better the de-noising effect.

In addition to the  $SNR$  and the  $RMSE$  in this paper we also use smoothness ( $r$ ) and cross-correlation coefficient ( $R$ ) to evaluate the signal denoising effect. They are defined as follows:

$$r = \frac{\sum_{t=1}^{t=n-1} [\hat{s}(t+1) - \hat{s}(t)]^2}{\sum_{t=1}^{t=n-1} [s(t+1) - s(t)]^2} \quad (7)$$

$$R = \frac{\sum_{t=1}^{t=n} [s(t) - \bar{s}(t)] [\hat{s}(t) - \bar{\hat{s}}(t)]}{\left\{ \sum_{t=1}^{t=n} [s(t) - \bar{s}(t)]^2 \sum_{t=1}^{t=n} [\hat{s}(t) - \bar{\hat{s}}(t)]^2 \right\}^{1/2}} \quad (8)$$

where,  $\bar{s}(t)$  is the mean value of  $s(t)$ , and  $\bar{\hat{s}}(t)$  is the mean value of  $\hat{s}(t)$ . Smoothness represents the ratio of the variance root between the first-order difference of the denoised signal and the first-order difference of the original signal. It reflects the low-frequency approximation information of the signal. The smaller the smoothness value, the better. The cross-correlation coefficient measures the similarity between the original signal and the denoised signal, and the larger the value, the better.

#### B. THE IMPROVED THRESHOLD FUNCTION

The basic idea of the hard threshold and soft threshold denoising methods is to remove relatively small wavelet coefficients as much as possible, and directly retain or shrink the relatively large wavelet coefficients. In hard threshold filtering, the estimation of wavelet coefficients is unbiased, but large oscillations (Gibbs phenomenon) are easily generated at the abrupt changes of signals after filtering. In soft threshold filtering, the estimation of wavelet coefficients is biased (the amplitude of wavelet coefficients whose amplitude is greater than the threshold value is partially subtracted, so the estimated mathematical expectation is not equal to the mathematical expectation of the observed value), and the filtered signal is too smooth.

To solve the problems of the traditional hard threshold and soft threshold functions, this paper proposes an improved threshold function. The improved threshold function is defined as :

$$\hat{w}_{i,j} = \begin{cases} w_{i,j} - w_{i,j}/[2 \exp(|w_{i,j}| - \lambda)], & |w_{i,j}| \geq \lambda \\ (w_{i,j}/2) \exp(|w_{i,j}| - \lambda), & |w_{i,j}| < \lambda \end{cases} \quad (9)$$

The function  $f(w_{i,j}) = \hat{w}_{i,j}$  is constructed, and to verify its feasibility in theory, its properties are investigated from the aspects of parity, continuity, asymptote, and constant difference calculation.

① Function continuity. Firstly the continuity of function is discussed on the positive half axis.

$$\begin{aligned} & \lim_{w_{i,j} \rightarrow \lambda^+} f(w_{i,j}) \\ &= \lim_{w_{i,j} \rightarrow \lambda^+} \{w_{i,j} - w_{i,j}/[2 \exp(w_{i,j} - \lambda)]\} \\ &= \lambda/2, \\ & \lim_{w_{i,j} \rightarrow \lambda^-} f(w_{i,j}) \\ &= \lim_{w_{i,j} \rightarrow \lambda^-} [(w_{i,j}/2) \exp(w_{i,j} - \lambda)] \\ &= \lambda/2 \\ &= \lim_{w_{i,j} \rightarrow \lambda^+} f(w_{i,j}) \end{aligned} \quad (10)$$

According to the definition of continuity, it can be concluded that  $f(w_{i,j})$  is continuous at  $w_{i,j} = \lambda$ . It can be seen from the discussion in ② below that  $f(w_{i,j})$  is an odd function, so it is continuous at  $w_{i,j} = -\lambda$ . The continuity of the function



can reduce the vibration of the reconstructed signal caused by the discontinuity of the hard threshold function.

② Function parity. The definition domain of the function is  $\mathbb{R}$  and  $f(-w_{i,j}) = -f(w_{i,j})$  is satisfied, so the function is an odd function, which is consistent with the soft threshold function and the hard threshold function.

③ Function asymptote. When  $|w_{i,j}| \geq \lambda$ , there is:

$$\lim_{w_{i,j} \rightarrow \infty} [f(w_{i,j})/w_{i,j}] = 1 - 1/\lim_{w_{i,j} \rightarrow \infty} [2 \exp(|w_{i,j}| - \lambda)] = 1 \quad (11)$$

According to (11), when  $|w_{i,j}| \geq \lambda$ , the asymptote of  $f(w_{i,j})$  is  $f(w_{i,j}) = w_{i,j}$ , and the asymptote coincides with the hard threshold function.

④ Constant difference calculation. The calculation formula of constant difference is:

$$\begin{aligned} \lim_{w_{i,j} \rightarrow \infty} [f(w_{i,j}) - w_{i,j}] &= \lim_{w_{i,j} \rightarrow \infty} \{w_{i,j} - w_{i,j}/[2 \exp(|w_{i,j}| - \lambda)] - w_{i,j}\} \\ &= 0 \end{aligned} \quad (12)$$

Since the ultimate goal of threshold quantization of high-frequency coefficients of wavelet decomposition is to make  $\|w_{i,j} - w_{i,j}\|$  as small as possible, it can be seen from (12) that this condition is met.

The threshold function curve is shown in Fig. 3.

### C. WAVELET DE-NOISING BASED ON IMPROVED THRESHOLD FUNCTION

The specific process of wavelet transform with improved threshold function denoising algorithm for gas-holdup signal of optical fiber probe is as follows.

① The input noisy gas-holdup signal is wavelet transformed to obtain the multi-layer wavelet decomposition signal.

② The coefficients of the high-frequency part of the wavelet decomposition signal at each layer are filtered by using the improved threshold function (9).

③ The reconstructed signal is obtained by an inverse wavelet transform of the filtered signal.

## IV. EXPERIMENT AND RESULT ANALYSIS

### A. SYNTHETIC SIGNAL DENOISING EXPERIMENT

Before the formal denoising of the optical fiber gas-holdup signal, a simulation experiment was conducted using the bumps signal for noise removal simulation verification, and analyzing the experimental results to provide a reference experience for processing the real signal. In order to better approximate the actual signal of the optical fiber gas-holdup, the bumps signal is used as the analog signal in the simulation experiment, and the original pure signal is shown in Fig. 4. Add noise to the analog signal. The zero mean white noise sequence is used to simulate the additional noise of the optical fiber probe gas-holdup meter. Set the signal-to-noise ratio being 4. The signal sequence containing noise is shown in Fig. 5.

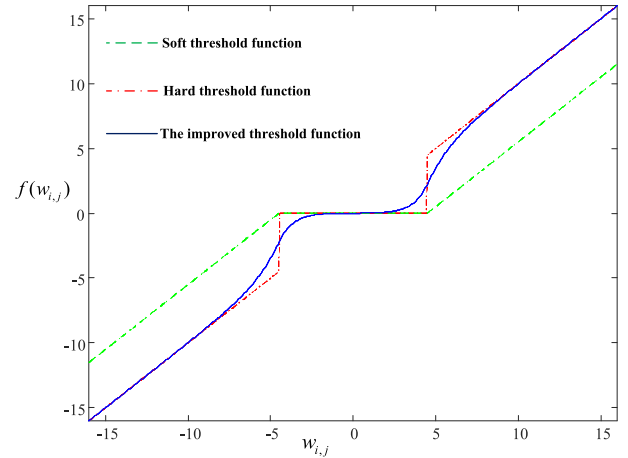


FIGURE 3. Threshold function curve.

After several experiments, comparison, and selection, db8 is selected as the wavelet basis function, and the number of decomposition layers is 7. Four threshold selection methods are used to de-noise the above noisy signal, and the de-noising effect is compared: ① Soft threshold estimation based on Stein unbiased likelihood estimation (Rigsure); ② Length logarithmic threshold (Sqrtwolong); ③ Heuristic SURE threshold (Heure); ④ Minimax variance threshold (Minimaxi). Using the soft threshold function, the de-noising results of four different threshold selection methods are shown in Fig. 6.

Compared with the soft and hard threshold function wavelet transform denoising methods, the improved threshold function wavelet transform method is used to denoise, and its effect is shown in Fig. 7.

Under the db8 wavelet basis function, the soft threshold function and the hard threshold function are used to calculate the root mean square error, the signal-to-noise ratio, smoothness, and cross-correlation coefficient of the simulated signal after de-noising by the four threshold selection methods, as a comparison, the above indicators of the noisy signal are calculated, as well as after de-noising by the improved threshold function wavelet transform method. The results are shown in Table 1.

In table 1 it shows the following points:

① The SNR of the noisy signal is 3.8715, the corresponding RMSE value is 0.9585, the smoothness value  $r$  is 38.0926, cross-correlation coefficient value  $R$  is 0.9024. No matter which method is used for de-noising, the SNR value of the signal after de-noising will increase to varying degrees, and the corresponding RMSE value will decrease to varying degrees. This shows that no matter which de-noising method is used, it can de-noise to a certain extent, but the de-noising effect is different.

② Among the four different threshold selection methods, for the hard threshold function, the de-noising effect of the Sqrtwolong method is the best. For example, the SNR of the Sqrtwolong method is 6.8195, which is larger than that of

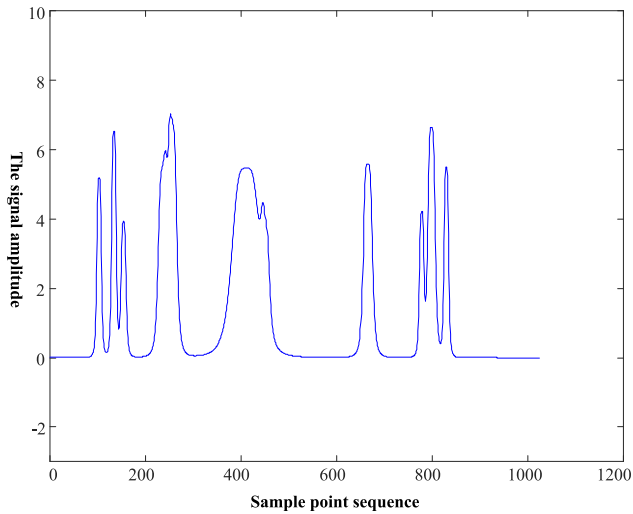


FIGURE 4. The original pure signal.

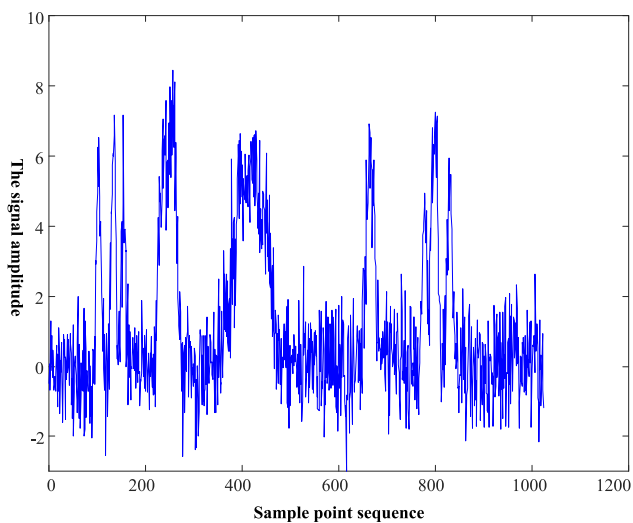


FIGURE 5. The signal sequence containing noise.

the other three methods, and the  $RMSE$  value of this method is 0.4862, which is smaller than that of the other three methods. For the improved threshold function method, the de-noising effect of the Sqtwolong method is also the best. However, for the soft threshold function, the de-noising indicators corresponding to the four different threshold selection methods have their own advantages and disadvantages. For example, the smoothness of the Sqtwolong method is 0.3469, which is smaller than that of the other three methods. The correlation coefficient value of the Minimaxi method is 0.9692, which is larger than that of the other three methods. To sum up, among the four different threshold selection methods, the Sqtwolong method has a better de-noising effect.

③ Among all the 12 de-noising methods above, the Sqtwolong threshold selection method of improved threshold function wavelet transform is the best in almost every index, except for the smoothness index, which is slightly worse. The  $SNR$  of this method is 7.2465, the corresponding  $RMSE$  value

TABLE 1. The de-noising effect of different kinds of threshold methods.

The index		$SNR$	$RMSE$	$r$	$R$
Signal					
Noisy signal		3.8715	0.9585	38.0926	0.9024
Soft-threshold	Rigrsure	6.5552	0.5167	7.8754	0.9661
	Sqtwolog	5.2326	0.7006	0.3469	0.9452
	Heursure	6.5552	0.5167	7.8754	0.9661
	Minimaxi	6.5030	0.5229	0.6736	0.9692
Hard-threshold	Rigrsure	4.187	0.8914	32.0606	0.9137
	Sqtwolog	6.8195	0.4862	0.9059	0.9702
	Heursure	4.187	0.8914	32.0606	0.9137
	Minimaxi	6.4766	0.5261	6.7036	0.9661
The improved threshold	Rigrsure	5.0985	0.7226	20.3992	0.9401
	Sqtwolog	7.2465	0.4407	1.1256	0.9754
	Heursure	5.0985	0.7226	20.3992	0.9401
	Minimaxi	6.9871	0.4678	5.6272	0.9729

is 0.4407, the smoothness value is 1.1256, and the correlation coefficient value is 0.9754. This shows that the improved threshold function wavelet transform method proposed in this paper selects the Sqtwolong threshold method for a better de-noising effect. Therefore, we choose this method for de-noising in the subsequent processing of optical fiber gas-holdup signal.

In order to further evaluate the denoising effect of the improved threshold function wavelet transform method based on Sqtwolong, we also discussed the cross-wavelet transform. We compare the time-frequency structure of the denoised and original data by performing a cross-wavelet transform. The XWT is constructed from the wavelet coefficients of the original signal ( $s$ ) and the denoised signal ( $\hat{s}$ ) and will expose their common power and relative phase in time–frequency space. The XWT measures the similarity of the wavelet representations of two signals and provides the ability to account for temporal (or spatial) variability in spectral character. Following Torrence and Compo [25], the XWT is defined as:

$$XWT = s \times \hat{s}^* \quad (13)$$

in which  $*$  denotes complex conjugation. The higher the value of XWT, the greater the correlation between  $s$  and  $\hat{s}$ .

High-power areas in Fig. 8 indicate the correlation of high-magnitude coefficients in the denoised and original spectrums. The XWT shows that the two waveforms are in phase in all the sectors with significant common power (Fig. 8). Outside of the area with significant power the phase relationship is complicated. This shows that a strong link exists between the denoised and original data.

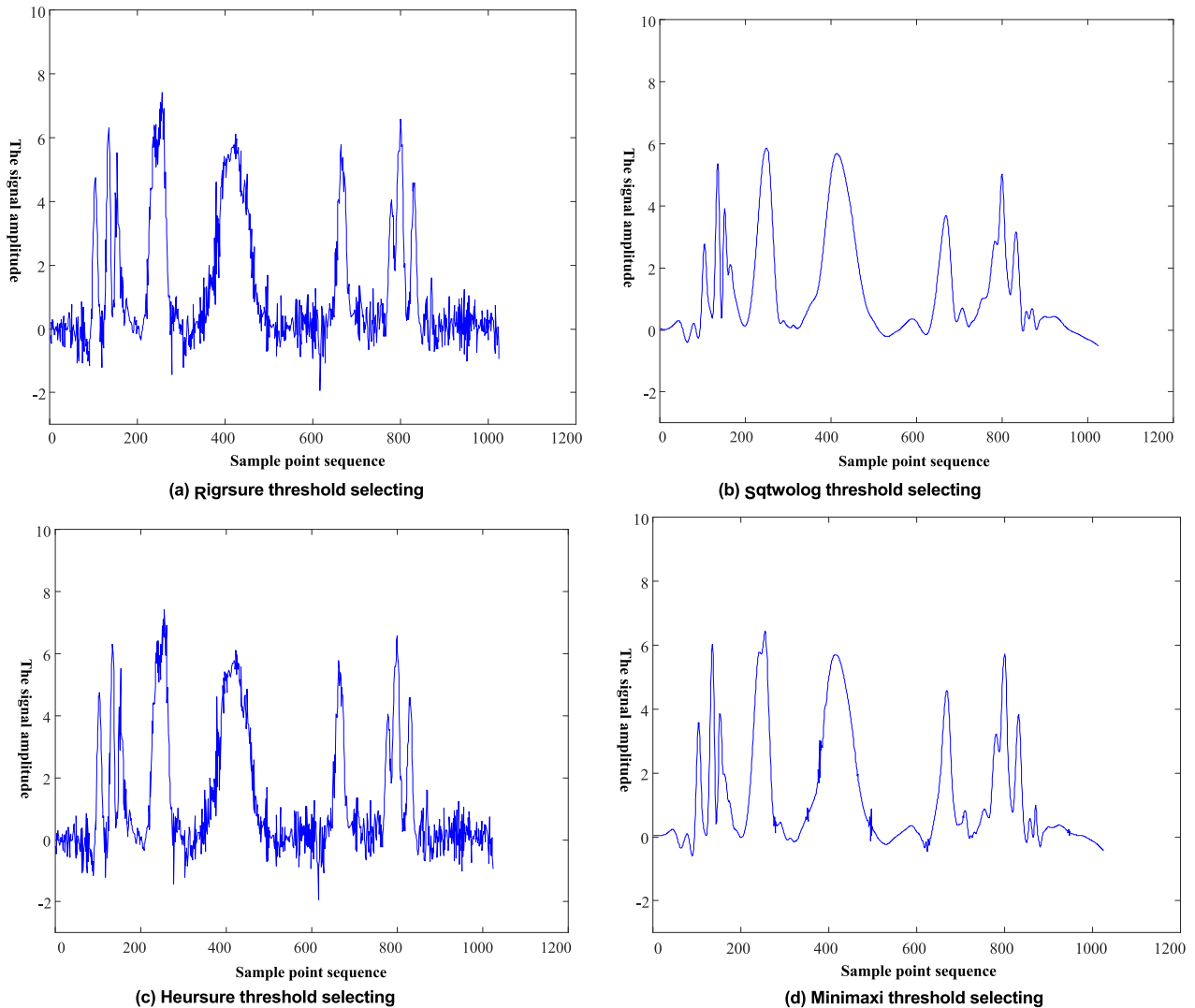


FIGURE 6. The de-noising effect of four different threshold selection methods.

### B. THE OPTICAL FIBER GAS-HOLDUP SIGNAL DENOISING EXPERIMENT

The structure of the optical fiber gas-holdup meter measurement system in this paper is shown in Fig. 9. The optical fiber gas-holdup meter is used to measure the local gas-holdup signal in the multiphase flow pipeline, and the data acquisition card is used to transmit it to the upper computer, and the data of the gas-holdup signal is denoised and analyzed.

The signal sampling rate of the measurement system is 2000Hz, the number of sampling points per frame is 1024, and the reference voltage of the AD acquisition unit is  $V_{REF+} = 3.3V$ ,  $V_{REF-} = 0V$ . The AD conversion accuracy is 12 bits, that is, the amplitude range of the AD acquisition signal is 0~4095. The gas-holdup signal of oil-gas-water three-phase flow in the well downhole acquired and output by the optical fiber gas-holdup meter in real time is shown in Fig. 10.

After several experiments, db8 is selected as the wavelet basis function, and the number of decomposition layers is 7. Four threshold methods are used to de-noise the gas-holdup signal of the fiber probe to compare the de-noising effect: ① Soft threshold estimation based on Stein unbiased likelihood estimation (Rigsure); ② Length logarithmic threshold (Sqtwolog); ③ Heuristic SURE threshold (Heursure); ④ Minimax variance threshold (Minimaxi). And for the soft-threshold function method, the de-noising result is shown in Fig. 11.

To investigate the de-noising effect of different methods, and quantify the de-noising indicators:  $SNR$ ,  $RMSE$ , smoothness, and correlation coefficient, a pure signal without noise is required. In the actual gas-holdup signal processing of the optical fiber, because the pure signal cannot be obtained, we have to replace the pure signal with the denoised signal to calculate each de-noising index as an approximate estimate, which provides some reference for the de-noising

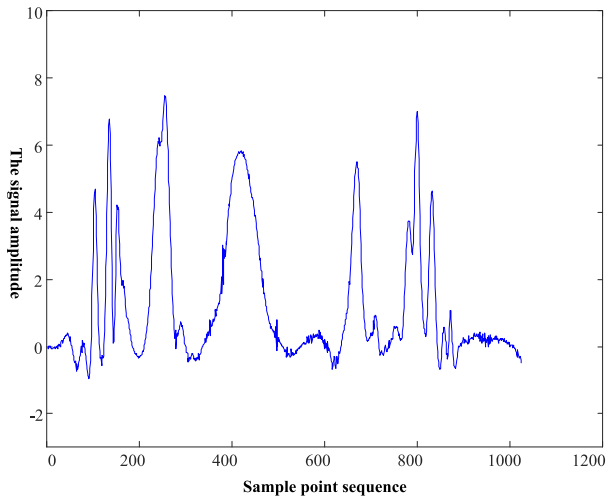


FIGURE 7. De-noising effect of wavelet transform with improved threshold function.

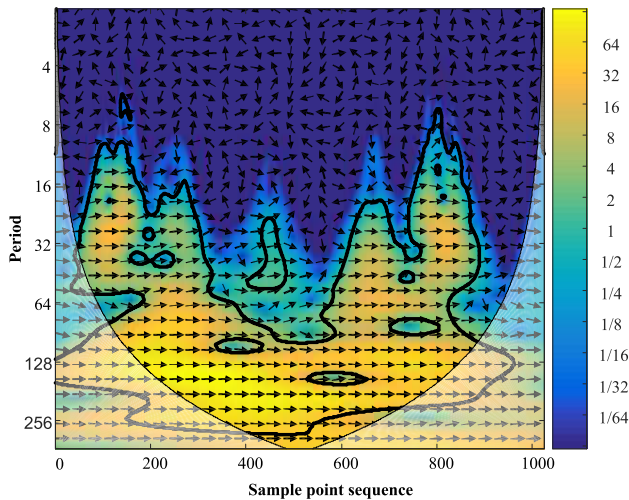


FIGURE 8. The cross-wavelet transform (XWT) of the original and denoised data. The phase arrows show the relative phasing of the two time series. Arrows pointing right: in-phase, left: antiphase, down: original phase leading the denoised phase by 90°, and up: denoised phase leading original phase by 90°. The color version of this figure is available only in the electronic edition.

effect. Under the db8 wavelet basis function, for the noisy optical fiber gas-holdup signal, each de-noising index after de-noising by four kinds of threshold selection methods is calculated, as shown in Table 2.

In Table 2, the SNR of Minimaxi is 31.9999, which is larger than that of the other three methods. Meanwhile, the RMSE of Minimaxi is 0.5229, which is smaller than that of the other three methods. Compared with the Minimaxi selection method, the indexes of the Sqrtwolong method are slightly worse. In addition, Table 1 in section III-A quantitatively verified the superiority of the length logarithmic threshold (Sqrtwolong) method in the simulation signal processing among the above four threshold de-noising methods. In comprehensive consideration, for the gas-holdup signal

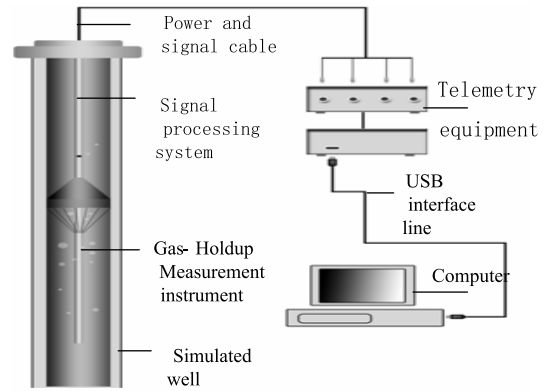


FIGURE 9. The system structure of measuring gas-holdup by optical fiber probe.

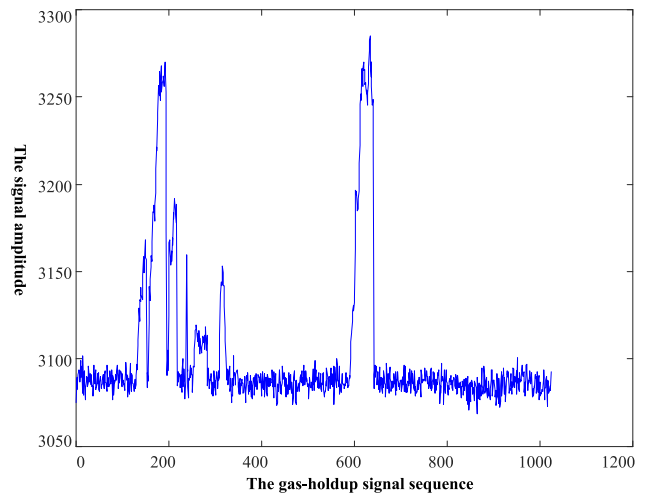


FIGURE 10. The original gas-holdup signal of the optical fiber probe.

TABLE 2. The de-noising effect of soft-threshold of four kinds of threshold methods.

The index	Rigrsure	Sqrtwolog	Heursure	Minimaxi
SNR	19.5819	30.1509	30.1509	31.9999
RMSE	34.1556	2.9962	2.9962	0.5229
r	0.0011	0.5886	0.5886	0.7141
R	0.5732	0.9976	0.9976	0.999

de-noising of the optical fiber, the length logarithmic threshold (Sqrtwolong) method is better.

Through the above experimental comparison, the length logarithmic threshold (Sqrtwolong) method is selected as the de-noising threshold in this paper, and three methods: hard threshold function, soft threshold function, and improved threshold function are respectively used to de-noise the gas-holdup signal of the optical fiber probe. The de-noising effect is shown in Fig. 12.

The de-noising evaluation indexes of the above three threshold functions for the actual optical fiber gas-holdup



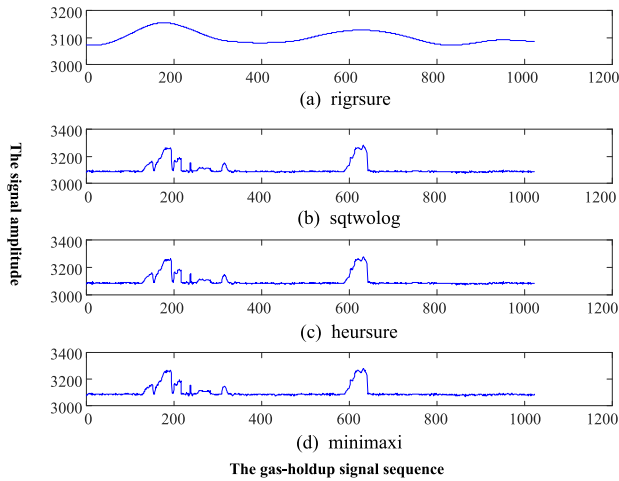


FIGURE 11. De-noising results using four kinds of threshold methods.

TABLE 3. Indicator values after de-noising by three kinds of threshold functions.

The index	Hard threshold	Soft threshold	The improved threshold
<i>SNR</i>	33.4041	30.1509	34.1393
<i>RMSE</i>	1.4166	2.9962	1.196
<i>r</i>	0.9599	0.5886	0.9326
<i>R</i>	0.9994	0.9976	0.9996

meter signal are calculated(In the calculation, the pure signal was replaced by the de-noised signal, and each de-noising index was calculated as an approximate estimate to provide some reference for the de-noising effect.), and the results are shown in Table 3.

By comparing three different threshold de-noising methods in Fig. 11 and Table 3, it can be seen that:

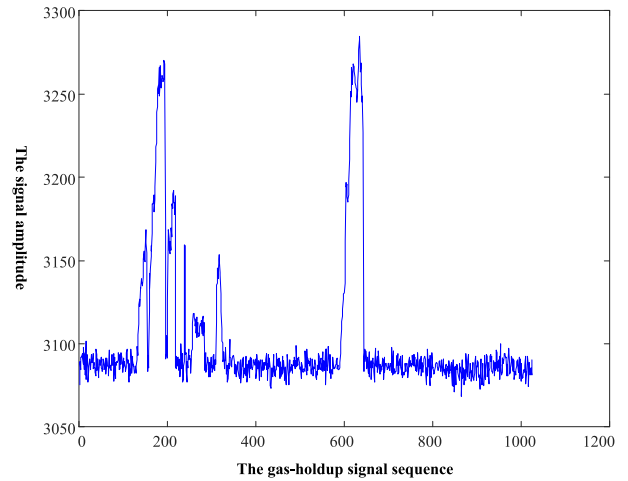
① Hard threshold, soft threshold, and improved threshold methods all can de-noise the original signal to a certain extent.

② The result of hard threshold processing is relatively rough. Although it preserves the edge local characteristics of the original signal to a certain extent, it is mixed with the noise signal, which affects the quality of the reconstructed signal and lacks flexibility.

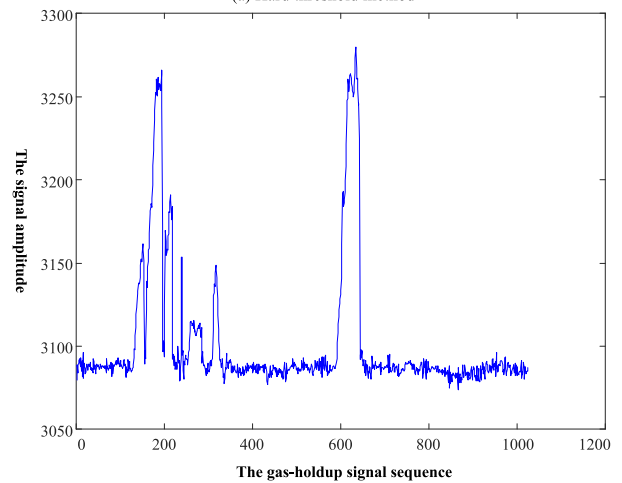
③ The soft threshold processing results are relatively ideal, overcoming the defects of hard threshold processing to some extent, and the overall continuity is good and relatively smooth.

④ The improved threshold processing results are the most ideal, compared with soft threshold and hard threshold de-noising. And the improved threshold de-noising method eliminates more noise signals while retaining the local edge features of the original signal, so the de-noising effect is more obvious.

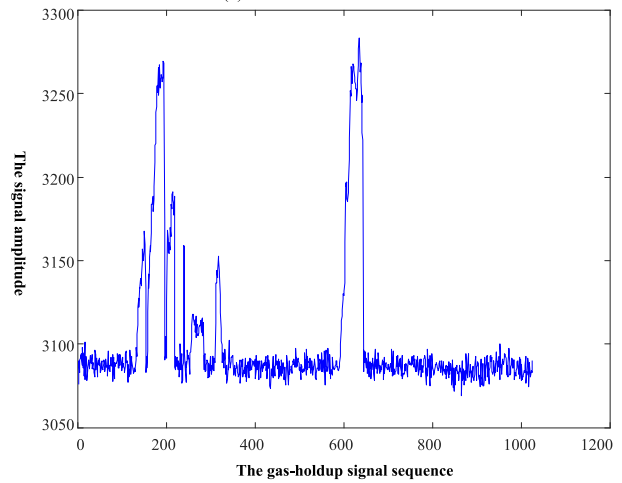
⑤ Compared with hard and soft threshold processing, the improved threshold processing has a higher *SNR* value and smaller *RMSE* value, and it has a better de-noising effect.



(a) Hard threshold method



(b) Soft threshold method



(c) The improved threshold method

FIGURE 12. Effect of three threshold methods for de-noising gas-holdup signal.

In terms of local gas-holdup, due to the existence of interfacial tension, the output signal of the optical fiber probe is usually not a regular rectangular wave, but an approximate trapezoidal wave. Therefore, it is necessary to convert the trapezoidal wave into a rectangular wave by setting the

**TABLE 4. The comparison on gas ratio and amplitude of signal before and after de-noising.**

Signal	Maximum amplitude	Minimum amplitude	Threshold	Gas ratio
Original signal	3285	3068	3133	120/1024
Hard threshold	3284	3068	3133	120/1024
Soft threshold	3279	3073	3135	117/1024
The improved threshold	3283	3069	3133	120/1024

threshold value to accurately determine the time when bubbles or air masses pass through the probe head and obtain the local section gas-holdup. In this paper, the single threshold method is used to process the gas-holdup signal of the optical fiber probe. In Table 4, the proportion of the gas phase in the oil-gas-water three-phase flow is shown.

It can be seen from Table 4 that the parameters of the signal after de-noising with the improved threshold function are very close to those of the original signal. The parameters of the signal after de-noising with the hard threshold function are basically consistent with the improved threshold function. By comparison, the performance of the soft threshold function after de-noising is slightly worse.

To sum up, it can be seen that the signal processing of the optical fiber gas-holdup meter is verified again, and it is feasible to use the improved threshold function to de-noise. At the same time, the improved threshold function de-noising has a higher SNR value and smaller RMSE value and has a better de-noising effect.

## V. DISCUSSION

Aiming at the defects of hard and soft threshold functions in the existing wavelet threshold denoising, this paper proposes an improved threshold function. The improved threshold function is between the hard threshold function and the soft threshold function. It has the advantages of both hard and soft threshold algorithms, and can well retain the local edge features of the original signal. At the same time, it can effectively overcome the discontinuity of the hard threshold method and the constant bias of the soft threshold method.

The wavelet transform based on the improved threshold function is used to de-noise the signal of the optical fiber gas-holdup meter. Through experiment, it verifies the validity of this method in the signal denoising of the optical fiber gas-holdup meter. The experimental results show that compared with the hard and soft threshold functions, the output SNR value of the proposed method is larger, the RMSE value is

smaller, and the denoising effect is better. At the same time, the original features of the gas-holdup measuring signal are better preserved, which provides a reference for the signal processing and dynamic monitoring analysis of the subsequent oil well downhole production.

## REFERENCES

- [1] X. Shi, C. Tan, F. Dong, and Y. Murai, "Oil-gas-water three-phase flow characterization and velocity measurement based on time-frequency decomposition," *Int. J. Multiphase Flow*, vol. 111, pp. 219–231, Feb. 2019.
- [2] P. Sassi, G. Fernández, Y. Stiriba, and J. Pallarès, "Effect of solid particles on the slug frequency, bubble velocity and bubble length of intermittent gas-liquid two-phase flows in horizontal pipelines," *Int. J. Multiphase Flow*, vol. 149, Apr. 2022, Art. no. 103985.
- [3] S. Harjanto, D. Haryono, H. Nugraha, G. Saputra, M. R. Baidillah, M. Al Huda, and W. P. Taruno, "Gas holdup and bubble flow transition characteristics in column flotation process determined by capacitive signals measurement," *Brazilian J. Chem. Eng.*, vol. 38, no. 2, pp. 361–372, Jun. 2021.
- [4] W. Ren, N. Jin, and J. Zhang, "Modelling of ultrasonic method for measuring gas holdup of oil-gas-water three phase flows," *Ultrasonics*, vol. 124, Aug. 2022, Art. no. 106740.
- [5] M. Mokhtari and J. Chaouki, "New technique for simultaneous measurement of the local solid and gas holdup by using optical fiber probes in the slurry bubble column," *Chem. Eng. J.*, vol. 358, pp. 831–841, Feb. 2019.
- [6] X. Guo, L. Kong, and Y. Zhang, "Logging equipment for void fraction of oil-gas-water three-phase flow based on optical fiber sensor," *Electron. Technol.*, vol. 37, no. 2, pp. 68–70, 2010.
- [7] H. Yerranna, K. S. Kumar, and S. L. Sabat, "Phase noise modeling and experimental demonstration of single and dual-loop direct modulation optoelectronic oscillator," *IEEE J. Quantum Electron.*, vol. 58, no. 6, pp. 1–10, Dec. 2022.
- [8] P. Flandrin, P. Gonçalves, and G. Rilling, "EMD equivalent filter banks, from interpretation to applications," in *Hilbert-Huang Transform and Its Applications*. NJ, USA: World Scientific, 2005, pp. 57–74.
- [9] A. O. Boudraa and J. C. Cexus, "Denoising via empirical mode decomposition," in *Proc. IEEE ISCCSP*, vol. 4, Mar. 2006.
- [10] B. Cai, Z. Wang, H. Zhu, Y. Liu, K. Hao, Z. Yang, Y. Ren, Q. Feng, and Z. Liu, "Artificial intelligence enhanced two-stage hybrid fault prognosis methodology of PMSM," *IEEE Trans. Ind. Informat.*, vol. 18, no. 10, pp. 7262–7273, Oct. 2022.
- [11] B. Weng, M. Blanco-Velasco, and K. E. Barner, "ECG denoising based on the empirical mode decomposition," in *Proc. Int. Conf. IEEE Eng. Med. Biol. Soc.*, Aug. 2006, pp. 1–4.
- [12] K. Khaldi, M. Turki-Hadj Alouane, and A.-O. Boudraa, "A new EMD denoising approach dedicated to voiced speech signals," in *Proc. 2nd Int. Conf. Signals, Circuits Syst.*, Nov. 2008, pp. 1–5.
- [13] G. S. Tsolis and T. D. Xenos, "Seismo-ionospheric coupling correlation analysis of earthquakes in Greece, using empirical mode decomposition," *Nonlinear Processes Geophys.*, vol. 16, no. 1, pp. 123–130, Feb. 2009.
- [14] Y.-X. Li and L. Wang, "A novel noise reduction technique for underwater acoustic signals based on complete ensemble empirical mode decomposition with adaptive noise, minimum mean square variance criterion and least mean square adaptive filter," *Defence Technol.*, vol. 16, no. 3, pp. 543–554, Jun. 2020.
- [15] J. Han and M. van der Baan, "Microseismic and seismic denoising via ensemble empirical mode decomposition and adaptive thresholding," *Geophysics*, vol. 80, no. 6, pp. KS69–KS80, Nov. 2015.
- [16] J. L. García-Franco, S. Osprey, and L. J. Gray, "A wavelet transform method to determine monsoon onset and retreat from precipitation time-series," *Int. J. Climatol.*, vol. 41, no. 11, pp. 5295–5317, Sep. 2021.
- [17] I. Daubechies, *Ten Lectures on Wavelets*. Philadelphia, PA, USA: Society for Industrial and Applied Mathematics, 2006.
- [18] J. B. Tary, R. H. Herrera, J. Han, and M. van der Baan, "Spectral estimation-what is new? What is next?" *Rev. Geophys.*, vol. 52, no. 4, pp. 723–749, Dec. 2014.
- [19] Y. Sang, D. Wang, J.-C. Wu, Q.-P. Zhu, and L. Wang, "Entropy-based wavelet de-noising method for time series analysis," *Entropy*, vol. 11, no. 4, pp. 1123–1147, 2009.

- [20] J. J. Galiana-Merino, "De-noising of short-period seismograms by wavelet packet transform," *Bull. Seismolog. Soc. Amer.*, vol. 93, no. 6, pp. 2554–2562, Dec. 2003.
- [21] A. C. To, J. R. Moore, and S. D. Glaser, "Wavelet denoising techniques with applications to experimental geophysical data," *Signal Process.*, vol. 89, no. 2, pp. 144–160, 2009.
- [22] P. K. Jain and A. K. Tiwari, "An adaptive thresholding method for the wavelet based denoising of phonocardiogram signal," *Biomed. Signal Process. Control*, vol. 38, pp. 388–399, Sep. 2017.
- [23] A. Antoniadis, "Wavelet methods in statistics: Some recent developments and their applications," *Statist. Surv.*, vol. 1, pp. 16–55, Jan. 2007.
- [24] A. Ansari, A. Noorzad, H. Zafarani, and H. Vahidifard, "Correction of highly noisy strong motion records using a modified wavelet denoising method," *Soil Dyn. Earthq. Eng.*, vol. 30, no. 11, pp. 1168–1181, Nov. 2010.
- [25] C. Torrence and G. P. Compo, "A practical guide to wavelet analysis," *Bull. Am. Meteorol. Soc.*, vol. 79, no. 1, pp. 61–78, 1998.



**SHUJUN CHEN** received the M.S. degree in software engineering from Yanshan University, China, in 2012. She is currently an Experimenter with the Teaching Technology Center, Hebei University of Engineering. Her research interests include data fusion and artificial intelligence.

• • •



**SHENGXUE DU** received the Ph.D. degree in computer application technology from Yanshan University, China, in 2016. He is currently a Teacher with the Department of Computer Science and Technology, Hebei University of Engineering. His research interests include data fusion, intelligent information processing, and machine learning.